High-Performance Intraoperative Cone-Beam CT on a Mobile C-Arm: An Integrated System for Guidance of Head and Neck Surgery

J. H. Siewerdsen,[a-e] M. J. Daly,[a] H. Chan,[a]
S. Nithiananthan,[b] N. Hamming,[c] K. K. Brock,[a,b,d] and J. C. Irish[e,f]

[a]Ontario Cancer Institute, Princess Margaret Hospital, Toronto ON
[b]Department of Medical Biophysics, University of Toronto, Toronto ON
[c]Institute of Biomaterials and Biomedical Engineering, University of Toronto, Toronto ON
[d]Department of Radiation Oncology, University of Toronto, Toronto ON
[e]Department of Otolaryngology – Head and Neck Surgery, University of Toronto, Toronto ON
[f]Department of Surgical Oncology Program, Princess Margaret Hospital, Toronto ON

ABSTRACT

A system for intraoperative cone-beam CT (CBCT) surgical guidance is under development and translation to trials in head and neck surgery. The system provides 3D image updates on demand with sub-millimeter spatial resolution and soft-tissue visibility at low radiation dose, thus overcoming conventional limitations associated with preoperative imaging alone. A prototype mobile C-arm provides the imaging platform, which has been integrated with several novel subsystems for streamlined implementation in the OR, including: real-time tracking of surgical instruments and endoscopy (with automatic registration of image and world reference frames); fast 3D deformable image registration (a newly developed multi-scale Demons algorithm); 3D planning and definition of target and normal structures; and registration / visualization of intraoperative CBCT with the surgical plan, preoperative images, and endoscopic video. Quantitative evaluation of surgical performance demonstrates a significant advantage in achieving complete tumor excision in challenging sinus and skull base ablation tasks. The ability to visualize the surgical plan in the context of intraoperative image data delineating residual tumor and neighboring critical structures presents a significant advantage to surgical performance and evaluation of the surgical product. The system has been translated to a prospective trial involving 12 patients undergoing head and neck surgery – the first implementation of the research prototype in the clinical setting. The trial demonstrates the value of high-performance intraoperative 3D imaging and provides a valuable basis for human factors analysis and workflow studies that will greatly augment streamlined implementation of such systems in complex OR environments.

Keywords: image-guided interventions, cone-beam CT, flat-panel detector, C-arm, 3D imaging, surgical navigation, image registration, head and neck surgery

1. INTRODUCTION

Head and neck (H&N) cancer surgery presents the challenge of infiltrative disease within complex 3D anatomy in proximity to a host of critical structures. This complexity is compounded by large population variations in anatomy and the high cost of failure associated with normal tissue complication. Of the four types of H&N lesions (neoplasms, orbital pathology, skull base defects, and inflammatory disease), conventional tracking and navigation relative to preoperative images is well suited only to a subset – viz., bony neoplasms.[1] Such systems are less useful for soft-tissue lesions prone to anatomical deformation (e.g., orbital herniation and masses infiltrating the nasopharynx and skull base), since they do not reflect intraoperative change. Performance in H&N surgery is thus often limited by a lack of geometric precision that could be resolved by high-performance intraoperative imaging capable of sub-mm 3D spatial resolution and soft-tissue visibility.

The need for precise 3D image guidance has motivated development of a mobile C-arm capable of cone-beam CT (CBCT).[2-17] Over the past several years, such a C-arm was developed in collaboration with Siemens Healthcare and investigated in a variety of surgical applications. By providing 3D image updates on demand, surgical navigation can be improved in a manner that properly accounts for anatomical deformation and excised tissue, thereby extending the role

Medical Imaging 2009: Visualization, Image-Guided Procedures, and Modeling,
edited by Michael I. Miga, Kenneth H. Wong, Proc. of SPIE Vol. 7261, 72610J

of image-guided surgery systems from rigid bony neoplasms to a broad spectrum of H&N interventions. As illustrated in Fig. 1, the CBCT C-arm is being incorporated in an integrated surgical guidance system that includes: the mobile C-arm for CBCT; real-time tracking; video endoscopy; volumetric planning; fast 3D deformable image registration; geometric registration of the current CBCT with preoperative images, prior CBCT images, and video endoscopy; and 3D visualization. This paper describes the development and integration of such subsystems for guidance of precision H&N surgery. The system has undergone extensive laboratory investigation in phantom, cadaver, and preclinical studies to evaluate the benefit to surgical performance and has recently entered prospective trials at our institution.

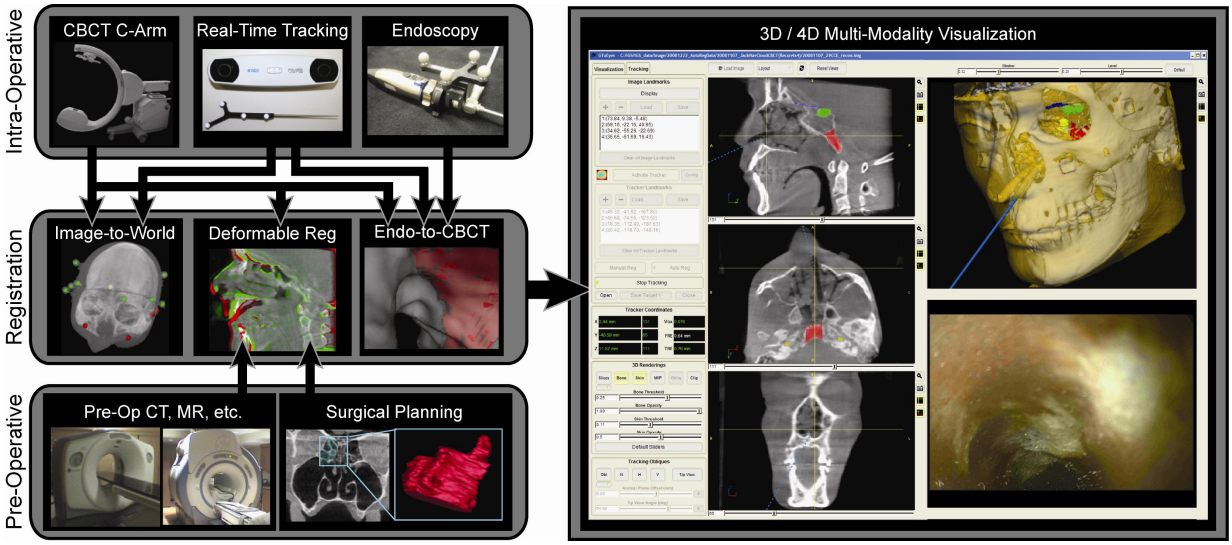

Figure 1. Flowchart illustration of systems for intraoperative C-arm CBCT surgical guidance. At left are illustrated intraoperative (top) and preoperative (bottom) processes integrated by means of geometric registration techniques, including: automatic image-to-world registration of CBCT and real-time tracking; deformable registration of CBCT with prior intraoperative CBCT, preoperative CT, and the surgical plan; and fusion / augmentation of CBCT volume images with video endoscopy. At right is illustrated a software interface for visualization of coregistered 3D images, video endoscopy, and surgical planning data.

2. INTEGRATION OF SUBSYSTEMS FOR CBCT-GUIDED SURGERY

2.1 Mobile C-Arm for Cone-Beam CT

A prototype CBCT imaging system based on a mobile isocentric C-arm (Siemens PowerMobil) has been developed in collaboration with Siemens Healthcare (Siemens SP, Erlangen Germany) as an experimental platform for pre-clinical application in image-guided surgery. As described previously[3] and illustrated in Fig. 2, the prototype C-arm was modified to include a large-area flat-panel detector (FPD, PaxScan 4030CB, Varian Imaging Products, Palo Alto CA) in place of the x-ray image intensifier, a motorized orbital drive, a method for geometric calibration, and a computer control system for image acquisition and 3D reconstruction. The system provides a volumetric field of view (~20 x 20 x 15 cm^3), and has demonstrated 3D image quality with sub-mm spatial resolution and soft-tissue visibility at low radiation dose (e.g., ~$^1/_{10}$ to $^1/_5$ the dose of a diagnostic CT scan). Volume reconstruction using a multi-threaded implementation of the FDK algorithm presents (256 x 256 x 192) voxel images within ~15 seconds of completing the scan, with future developments to include a GPU-based implementation and reconstruction simultaneous to projection acquisition such that 3D volumes are available immediately upon completing the scan.

The experimental prototype suggests a variety of advantages compared to existing commercially available 3D imaging systems. Compared to systems using an x-ray image intensifier as the image receptor, the prototype exhibits significantly improved spatial resolution, soft-tissue visibility, and a larger 3D FOV.[16] Compared to an enclosed gantry (e.g., a multi-detector CT scanner or a mobile platform in which the "C" is an enclosed "O"), the prototype preserves the flexible open geometry of a C-arm, with superior patient access for the surgeon and staff and improved line of sight for surgical tracking systems. Compared to a U-arm system that approaches from the superior end of the OR table, the C-arm is minimally obstructive to anesthesia, intubation, and monitoring systems and may remain at tableside during the procedure with little obstruction to patient access. Compared to ceiling-mounted C-arms, the mobile C-arm presents a relatively inexpensive platform that may be shared among multiple procedure rooms, the ICU, and emergency room.

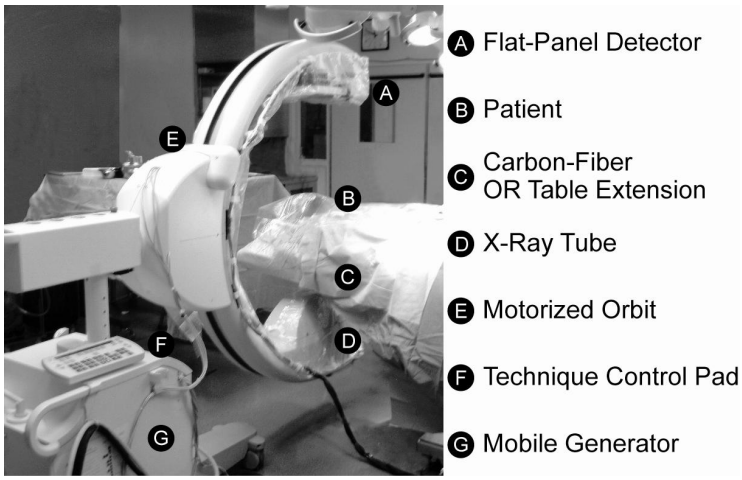

Figure 2. Photograph of the mobile C-arm for CBCT at tableside in head and neck surgery. Modifications to the (PowerMobil, Siemens Healthcare) platform include: a flat-panel detector, expansion of the FOV, added filtration appropriate to CBCT, motorized orbit, geometric calibration, and a computer control system for image acquisition and reconstruction.

2.2 Fast Deformable Image Registration

A system for fast 3D deformable image registration has been developed to transform preoperative images, the surgical plan (target and normal volumes), and other intraoperative CBCT images forward to the most recent intraoperative CBCT. A multi-scale Demons implementation[18] has been developed for accurately registering 3D CBCT volumes as illustrated in Fig. 3. A morphological pyramid [Fig. 3(a)] provides accurate registration on timescales consistent with intraoperative guidance (<10 sec at Pass 3: cross-correlation ~0.99, TRE <1-2 mm). Although head and neck anatomy presents a fairly rigid context, there is significant potential for deformation that cannot be resolved by rigid registration, owing to: *i*.) deformation of the target during the intervention; *ii*.) deformation of surrounding normal tissue (e.g., orbits) during target excision; and *iii*.) independent motion of rigid structures, such as the cranium, mandible, and spine.

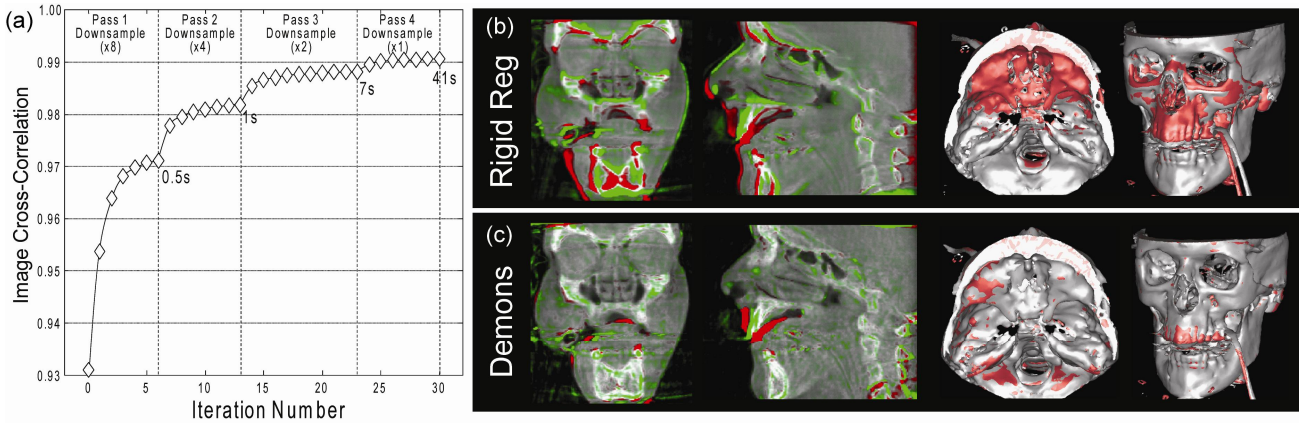

Figure 3. Illustration of 3D deformable registration. (a) Plot of cross-correlation between moving and target images over the course of multi-scale Demons registration. The algorithm converges within 7-40 sec and yields TRE <1-2 mm (measured in 7 anatomical landmarks). (b) Difference images (coronal and sagittal planes) and surface renderings illustrating registration of two CBCT images acquired during a sinus air cell excision. Rigid registration (cross-correlation ~0.93) fails to resolve deformation about the orbits, maxilla, mandible, and spine. (c) Demons registration (cross-correlation ~0.99) resolves such discrepancies.

2.3 Surgical Planning: Identification of Trajectory, Target, and Normal Structures

Preoperative planning is performed in diagnostic CT or, time-permitting, in CBCT acquired immediately prior to the procedure in the OR. An in-house system for 3D contouring of target and normal structures was developed using ITK-Snap (www.itksnap.org) allowing delineation in axial, sagittal, and/or coronal planes. Figure 4 illustrates example ethmoid and skull base targets delineated in CBCT-guided excision of a large soft-tissue tumor invading the paranasal sinuses. Combined with intraoperative CBCT and deformable registration, such planning permits evaluation of the surgical product and quantification of surgical performance (e.g., sensitivity and specificity of excised tissue). For example, Fig. 4(b) illustrates possible residual target (arrows) as soft tissue visualized in the post-excision CBCT scan residing within the planned target volume.

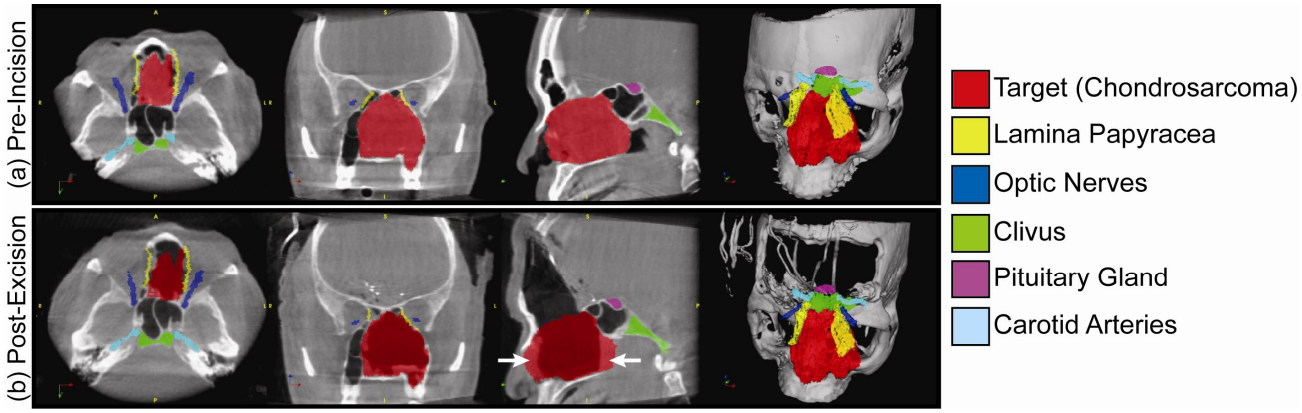

Figure 4. Example target volumes defined in CBCT-guided excision of a soft-tissue tumor invading the paranasal sinuses. Images in (a) illustrate the plan registered to an initial (pre-incision) CBCT image, with the target in red and surrounding landmarks and critical structures denoted. Images in (b) show target and normal volumes registered to an intraoperative CBCT acquired following tumor excision via anterior craniotomy. The arrows in the sagittal image denote possible residual tumor identified at the time of surgery.

2.4 Real-Time Tracking and Navigation

As illustrated in Fig. 5, an optical tracking system has been integrated with C-arm CBCT. The system presently incorporates a stereoscopic infrared camera (Polaris Vicra, NDI, Mississauga ON) and tracking of passive reflective markers on surgical instruments. A method for automatic registration of image and world reference frames is shown in Fig. 5(b), where segmentation of markers visible both to the camera and the C-arm (viz., reflective spheres containing a tungsten BB) combined with a knowledge of the C-arm geometry allows a complete 3D pose determination of fiducials to be computed directly from CBCT projection data. Such allows automatic registration in a manner that eliminates the conventional, time-consuming manual registration process. Knowledgeable selection of fiducial configuration is shown to minimize TRE [e.g., Fig. 5(c), TRE < 0.3 mm for pituitary target] and maximize TRE uniformity throughout the FOV.[19] Compared to the conventional manual technique, the automatic registration technique provides equivalent or superior TRE [Fig. 5(d)], superior reproducibility, improved workflow (seconds, instead of minutes), and automatic registration updates throughout the procedure with each CBCT scan. Furthermore, projection-based registration facilitates the development of novel fiducial configurations better suited to subcranial H&N surgeries without stereotactic frames or attachment to the cranium, requiring only that fiducials are visible within some subset of CBCT projections (but not necessarily constrained within the 3D FOV).

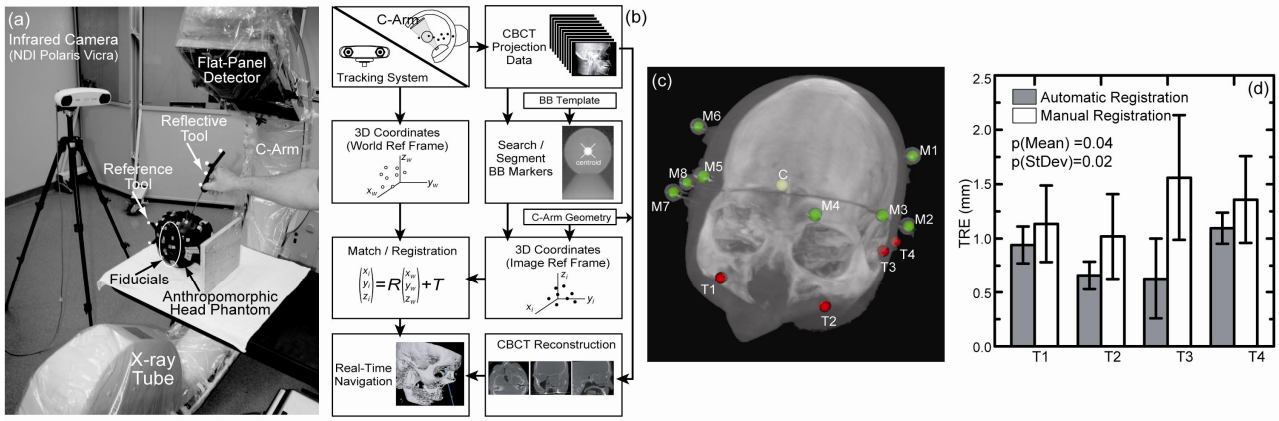

Figure 5. Illustration of tracking and navigation. (a) Experimental setup illustrating real-time tracking + CBCT in a head phantom. (b) Flowchart of method for automatic registration of image and world coordinate systems. (c) MIP image superimposed with an example fiducial configuration (M1-M8, green) the configuration centroid (C, yellow), and four anatomical targets (T1-T4, red). (d) TRE measured in targets T1-T4 for the automatic and conventional (manual) registration technique.

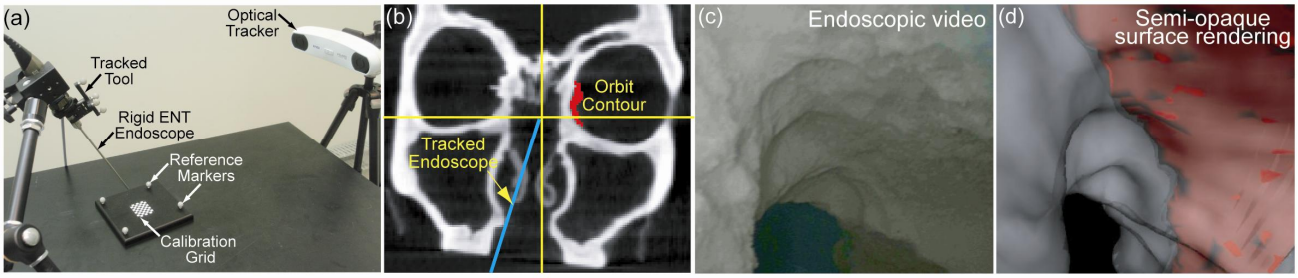

Figure 6. Tracking and fusion of video endoscopy with intraoperative CBCT. (a) Photograph of experimental setup. The endoscope is tracked by means of passive markers attached to the handle, with endoscope tip and orientation calibration by means of a reference tool and calibration grid. (b) Real-time tracking of the endoscope in the context of CBCT (coronal slice of a sinus phantom). Registration of (c) the endoscopic video image with 3D CBCT allows virtual or augmented reality images fused as in (d).

2.5 Tracking and Fusion of Endoscopic Video

Figure 6(a) illustrates a straight sinus endoscope (IMAGE1 camera with Hopkins II zero-degree scope, Karl Storz, Tuttlingen, Germany) modified to include infrared reflective markers for real-time tracking. The calibration method for determining the pose of the endoscope involves tracking the endoscope (the "tracked tool") during collection of 10 endoscopic images at various perspectives of a planar checkerboard grid (5x5 mm^2 squares) mounted on an optical reference tool. The intrinsic parameters (focal length, principal point, and distortion) and extrinsic parameters (translation and rotation) of the endoscope are determined using open-source software (Camera Calibration Toolbox for Matlab, available from the Open Source Computer Vision Library, CalTech[20]). The transformation between the coordinate systems of the endoscope tracked tool and the endoscope camera is determined from tracker tool measurements and extrinsic camera parameters registered in the calibration grid coordinate system. Registration of the endoscope position and orientation in the context of intraoperative CBCT [Fig. 5(b)] enables fusion of endoscopic video [Fig. 5(c)] with volumetric images – e.g., real-time visualization of 3D surface renderings from the perspective of the endoscope [Fig. 5(d)]. A number of options regarding video-CBCT fusion, triplanar CBCT slices at the endoscope tip, augmentation of video with CBCT images and planning data, and virtual reality representations of CBCT (e.g., surface renderings) can reveal anatomical structures not directly visible in the endoscopic view – e.g., critical structures obscured by blood or behind the visible anatomical surface.

Figure 7. Basic implementation of tableside 3D visualization. The surgeon interrogates intraoperative CBCT with the assistance of a technician to manipulate tri-planar views, tracked tool trajectories, 3D surface renderings, surgical planning data, and endoscopic video. Deployment of the CBCT guidance system in clinical trials allows investigation of how intraoperative 3D imaging can improve surgical decision making and how best to integrate systems in the OR without impeding surgical workflow.

2.6 Integration and Visualization of CBCT Guidance Systems

Incorporating each of the individual subsystems described above in a streamlined guidance system consistent with surgical workflow requirements presents a systems integration challenge, as does presenting multi-dimensional, multi-modality information to the surgeon in a manner that can be quickly interrogated to the benefit of surgical decision making. As illustrated in Fig. 1 (right panel), 3D visualization and navigation data are displayed via in-house software developed using the IGSTK library (Kitware Inc., Clifton Park NY). The current system (deployed in clinical trials as described below) allows 3D visualization of intraoperative CBCT, any prior CBCT or preoperative CT, MR, etc., real-time tracking of surgical instruments, and optional overlay of surgical planning data. Ongoing development of the research platform includes robust registration to preoperative CT, MR, and PET with augmented or virtual reality fusion of CBCT with video endoscopy. Figure 7 illustrates intraoperative use of the integrated display.

3. PRE-CLINICAL STUDIES

The benefit of CBCT guidance to surgical performance has been investigated in a series of phantom and cadaver studies involving a variety of challenging excision tasks performed with and without CBCT guidance. All cadaver studies were conducted in accordance with the Anatomy Act of Ontario. Such studies were critical to evaluating the potential benefit of CBCT guidance to H&N surgery, improving system integration, and facilitating a systematic translation to clinical trials. Within the specific context of H&N surgery, preclinical studies performed with the C-arm prototype include:

- Image quality and dose[4]
- Identification of CNS breach (CSF leak)[5] [see Fig. 8(a)]
- Tomosynthesis image quality,[6] localization accuracy,[7] and surgical excision performance[8]
- Access to the frontal recess[9]
- Temporal bone image quality[10] and visualization of cochlear implants[11]
- Surgical performance in skull base excision[12,13] [see Fig. 8(b)]

Such studies indicate a variety of qualitative and quantitative benefits to surgical performance, including improved orientation in the absence of clear anatomical landmarks, improved confidence in excision proximal to critical structures, and quantifiably improved accuracy of target ablation. For example, the ability to detect breach of the central nervous system (CNS) [causing cerebrospinal fluid (CSF) leak] was investigated using 5 cadavers in which breaches of various size and location were intentionally delivered. As illustrated in Fig. 8(a), CNS breach as small as 1-2 mm were confidently detected in intraoperative CBCT. The benefit of CBCT guidance to surgical performance was evaluated quantitatively in terms of sensitivity (fraction of target excised) versus specificity (fraction of normal preserved). As illustrated in Fig. 8(b), skull base ablation in cadaver models demonstrates a significant improvement in performance – superior sensitivity in target excision with CBCT guidance at any level of specificity.

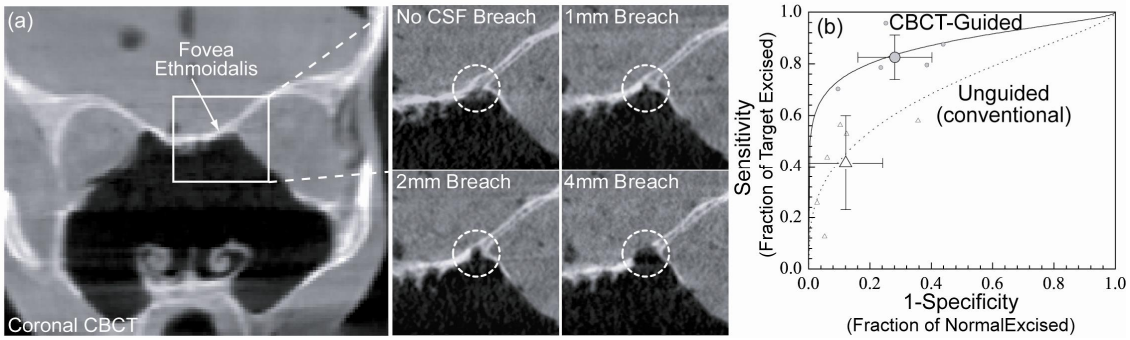

Figure 8. Surgical performance evaluation. (a) Qualitative assessment of improved confidence in excisions proximal to critical structures. CNS breach as small as 1-2 mm diameter could be confidently detected. (b) Quantitative evaluation of surgical performance in skull base ablation, showing a significant increase in performance under CBCT guidance.

4. DEPLOYMENT IN A CLINICAL TRIAL

Translation of the experimental prototype to prospective clinical trials is underway at our institution. The CBCT C-arm and associated IGS systems are being deployed under research protocol for the guidance of a variety of head and neck surgeries to evaluate in situ image quality, surgical performance, workflow, and human factors analysis. The research is conducted under informed consent according to IRB (REB) approved protocol and Health Canada Investigational Testing Authorization. Example images are shown in Fig. 9 for a case involving an esthesioneuroblastoma invading the nasal cavity, cribriform plate, and brain. The soft-tissue target could be directly delineated in CBCT, and intraoperative imaging demonstrated the clear potential for improved precision in such challenging excisions. Audio and video recordings combined with human factors analysis provide important guidance for streamlined integration of intraoperative image guidance within the complex environment of the OR in a manner that does not impede surgical workflow.

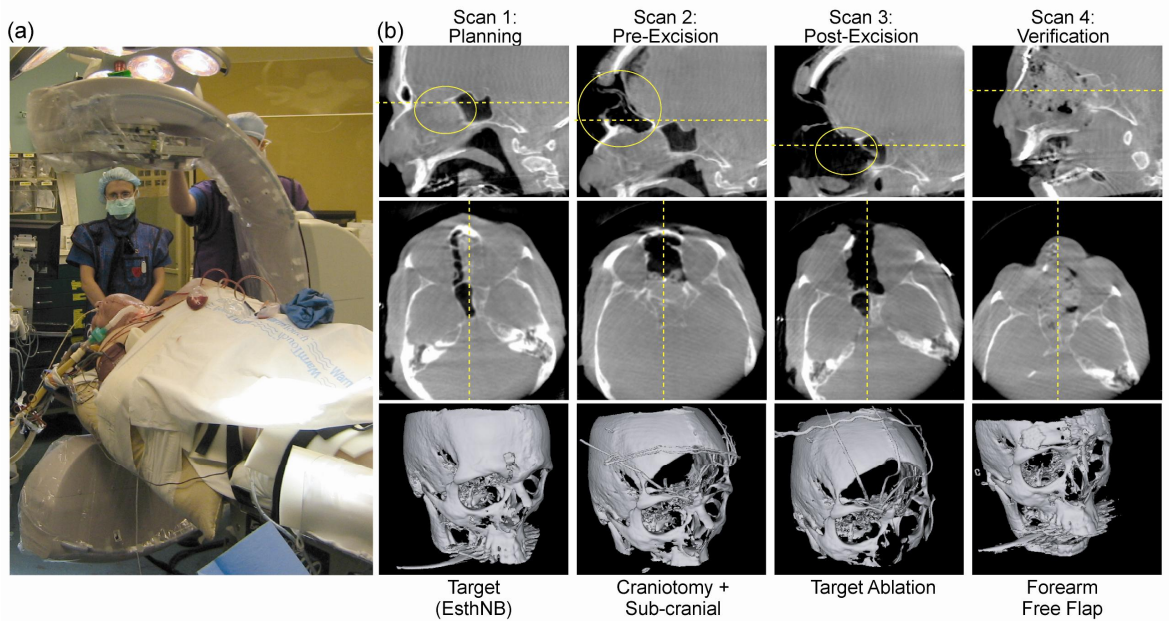

Figure 8. Illustration of the CBCT C-arm deployed in prospective trials. (a) Photograph of the C-arm in the OR. (b) Example CBCT images acquired at four stages of the procedure: 1.) prior to first incision, 2.) upon exposure of the surgical target, 3.) following target excision, and 4.) upon closure of the surgical field (verification).

5. CONCLUSIONS

The role of high-performance CBCT for image-guided interventions is rapidly emerging, with systems capable of sub-millimeter spatial resolution and soft-tissue visibility providing an important new modality for intraoperative visualization. A prototype C-arm for intraoperative CBCT imaging has demonstrated the potential improvement in surgical performance in laboratory studies, facilitating high-precision execution of challenging surgical tasks by resolving geometric uncertainty. In the context of head and neck surgery, such capability promises to broaden the application of image guidance beyond conventional boundaries (bony neoplasms) to the broad spectrum of H&N surgical targets, including infiltrative soft-tissue targets in proximity to critical structures amid a challenging architecture of deformable anatomy. The technical challenges associated with such capability are beyond 3D imaging alone and require streamlined integration of systems for imaging, deformable registration, surgical planning, real-time tracking of surgical tools, and 3D navigation / visualization of multi-dimensional, multi-modality data. The complexity of such technologies necessitates a systematic approach to integration combined with careful attention to human factors and surgical workflow to achieve successful clinical translation.

ACKNOWLEDGMENTS

The authors extend sincere appreciation to numerous individuals contributing to this program of research. The C-arm prototype was developed in collaboration with Siemens Healthcare (Siemens SP, Erlangen Germany), with special thanks to Dr. R. Graumann, Dr. K. Hermann, Dr. M. Mitschke, and Dr. D. Ritter. Surgeons and scientists in the Guided Therapeutics (GTx) Program (University Health Network) include Dr. A. Easty, Dr. D. Jaffray, Dr. M. Fehlings, Dr. M. Jewett, Dr. W. Kucharczyk, Dr. R. Weersink, and Dr. B. Wilson. Surgical fellows and residents (Otolaryngology – Head and Neck Surgery, University of Toronto) contributing to the work include Dr. G. Bachar, Dr. E. Barker, Dr. Y. Chan, Dr. M. Rafferty, and Dr. A. Vescan. The Surgical Skills Centre (Mt. Sinai Hospital, Toronto ON) assisted with cadaver studies, with thanks to Ms. D. Rego, Ms. M. Romanova, and Ms. L. Satterthwaite. Human factors analysis was conducted in collaboration with the Global eHealth Innovation Centre (University Health Network), with thanks to Ms. C. Banez, Mr. J. Cafazzo, and Ms. A. Cassano-Piche. The assistance of nursing, anesthesia, and surgical staff at the University Health Network (Toronto ON) is gratefully acknowledged, with special thanks to Ms. G. Gravely, Ms. K. McKinlay, and Ms. C. Simpson for assistance with the clinical trials. The work was supported by the Princess Margaret Hospital Foundation and the National Institutes of Health (R01-CA127944-02).

REFERENCES

1. R. Sindwani and R. D. Bucholz. "The next generation of navigational technology," Otolaryngol.Clin.North Am. 38[3]: 551-562 (2005).
2. J. H. Siewerdsen, D. A. Jaffray, G. K. Edmundson, W. P. Sanders, J. W. Wong, and A. Martinez. "Flat-panel cone-beam CT: A novel imaging technology for image-guided procedures," Proc.SPIE Visualization, Display, and Image-Guided Procedures 4319: 435-444 (2001).
3. J. H. Siewerdsen, D. J. Moseley, S. Burch, S. K. Bisland, A. Bogaards, B. C. Wilson, and D. A. Jaffray. "Volume CT with a flat-panel detector on a mobile, isocentric C-arm: pre-clinical investigation in guidance of minimally invasive surgery," Med Phys. 32[1]: 241-254 (2005).
4. M. J. Daly, J. H. Siewerdsen, D. J. Moseley, D. A. Jaffray, and J. C. Irish. "Intraoperative cone-beam CT for guidance of head and neck surgery: Assessment of dose and image quality using a C-arm prototype," Med Phys. 33[10]: 3767-3780 (2006).
5. G. Bachar, E. Barker, H. Chan, M. J. Daly, S. Nithiananthan, A. Vescan, J. C. Irish, and J. H. Siewerdsen. "Visualization of Anterior Skull Base Defects With Intraoperative Cone-Beam CT," Head and Neck Journal (submitted) (2009).
6. J. H. Siewerdsen, M. J. Daly, G. Bahar, D. J. Moseley, G. Bootsma, S. Chhabra, D. A. Jaffray, and J. C. Irish. "Multi-Mode C-Arm Fluoroscopy, Tomosynthesis, and Cone-Beam CT for Image-Guided Interventions: From Proof of Principle to Patient Protocols," Proc.SPIE Physics of Medical Imaging 6510: 65101A-1-A-11 (2007).
7. G. Bachar, J. H. Siewerdsen, M. J. Daly, D. A. Jaffray, and J. C. Irish. "Image quality and localization accuracy in C-arm tomosynthesis-guided head and neck surgery," Med Phys. 34[12]: 4664-4677 (2007).
8. G. Bachar, E. Barker, S. Nithiananthan, M. J. Daly, J. C. Irish, and J. H. Siewerdsen. "3D Tomosynthesis and Cone-Beam CT: A Fast, Low-Dose Intraoperative Imaging Technology for Guidance of Sinus and Skull Base Surgery," The Laryngosope (in press) (2009).
9. M. A. Rafferty, J. H. Siewerdsen, Y. Chan, D. J. Moseley, M. J. Daly, D. A. Jaffray, and J. C. Irish. "Investigation of C-arm cone-beam CT-guided surgery of the frontal recess," Laryngoscope 115[12]: 2138-2143 (2005).
10. M. A. Rafferty, J. H. Siewerdsen, Y. Chan, M. J. Daly, D. J. Moseley, D. A. Jaffray, and J. C. Irish. "Intraoperative cone-beam CT for guidance of temporal bone surgery," Otolaryngol.Head Neck Surg. 134[5]: 801-808 (2006).
11. E. Barker, K. Trimble, G. Bachar, S. Nithiananthan, M. J. Daly, J. C. Irish, and J. H. Siewerdsen. "C-Arm Cone-Beam CT for Verification of Cochlear Implants in the Abnormal Ear," J.Otolaryngol.Head Neck Surg. (accepted) (2009).
12. J. H. Siewerdsen, Y. Chan, D. J. Moseley, S. M. Kim, D. A. Jaffray, and J. A. Irish. "A Mobile, Isocentric C-Arm for Cone-Beam CT-Guided Head and Neck Tumor Surgery," Proc.SPIE Visualization, Display, and Image-Guided Procedures **5744**: 789-797 (2004).
13. Y. Chan, J. H. Siewerdsen, M. A. Rafferty, D. J. Moseley, D. A. Jaffray, and J. C. Irish. "Cone-beam computed tomography on a mobile C-arm: novel intraoperative imaging technology for guidance of head and neck surgery," J.Otolaryngol.Head Neck Surg. 37[1]: 81-90 (2008).
14. D. Ritter, J. Orman, C. Schmidgunst, and R. Graumann. "3D soft tissue imaging with a mobile C-arm," Comput.Med Imaging Graph. 31[2]: 91-102 (2007).
15. M. J. Daly, J. H. Siewerdsen, Y. B. Cho, D. A. Jaffray, and J. C. Irish. "Geometric calibration of a mobile C-arm for intraoperative cone-beam CT," Medical Physics 35[5]: 2124-2136 (2008).
16. A. Khoury, J. H. Siewerdsen, C. M. Whyne, M. J. Daly, H. J. Kreder, D. J. Moseley, and D. A. Jaffray. "Intraoperative cone-beam CT for image-guided tibial plateau fracture reduction," Comput.Aided Surg. 12[4]: 195-207 (2007).
17. A. Khoury, C. M. Whyne, M. Daly, D. Moseley, G. Bootsma, T. Skrinskas, J. Siewerdsen, and D. Jaffray. "Intraoperative cone-beam CT for correction of periaxial malrotation of the femoral shaft: a surface-matching approach," Med Phys. 34[4]: 1380-1387 (2007).
18. S. Nithiananthan, K. K. Brock, J. C. Irish, and J. H. Siewerdsen. "Deformable registration for intra-operative cone-beam CT guidance of head and neck surgery," Conf.Proc.IEEE Eng Med Biol.Soc. 1: 3634-3637 (2008).
19. N. M. Hamming, M. J. Daly, J. C. Irish, and J. H. Siewerdsen. "Effect of fiducial configuration on target registration error in intraoperative cone-beam CT guidance of head and neck surgery," Conf.Proc.IEEE Eng Med Biol.Soc. 1: 3643-3648 (2008).
20. Open Source Computer Vision Library. "Camera Calibration Toolbox for Matlab," www.vision.caltech.edu/bouguetj/calib_doc/ (2009).